Send Orders for Reprints to reprints@benthamscience.ae

Current Genomics, 2018, *19*, 179-191

REVIEW ARTICLE

Polytene Chromosomes – A Portrait of Functional Organization of the *Drosophila* Genome

Tatyana Yu Zykova[1], Victor G. Levitsky[2,3], Elena S. Belyaeva[1] and Igor F. Zhimulev[1,3,*]

[1]*Institute of Molecular and Cellular Biology of the Russian Academy of Sciences, Novosibirsk 630090, Russian Federation;* [2]*Institute of Cytology and Genetics of the Russian Academy of Sciences, Novosibirsk 630090, Russian Federation;* [3]*Novoisibirsk State University, Novosibirsk 630090, Russian Federation*

ARTICLE HISTORY

Received: December 31, 2015
Revised: April 01, 2016
Accepted: September 26, 2017

DOI:
10.2174/1389202918666171016123830

Abstract: This mini-review is devoted to the problem genetic meaning of main polytene chromosome structures – bands and interbands. Generally, densely packed chromatin forms black bands, moderately condensed regions form grey loose bands, whereas decondensed regions of the genome appear as interbands. Recent progress in the annotation of the *Drosophila* genome and epigenome has made it possible to compare the banding pattern and the structural organization of genes, as well as their activity. This was greatly aided by our ability to establish the borders of bands and interbands on the physical map, which allowed to perform comprehensive side-by-side comparisons of cytology, genetic and epigenetic maps and to uncover the association between the morphological structures and the functional domains of the genome.

These studies largely conclude that interbands 5'-ends of housekeeping genes that are active across all cell types. Interbands are enriched with proteins involved in transcription and nucleosome remodeling, as well as with active histone modifications. Notably, most of the replication origins map to interband regions. As for grey loose bands adjacent to interbands, they typically host the bodies of housekeeping genes. Thus, the bipartite structure composed of an interband and an adjacent grey band functions as a standalone genetic unit. Finally, black bands harbor tissue-specific genes with narrow temporal and tissue expression profiles. Thus, the uniform and permanent activity of interbands combined with the inactivity of genes in bands forms the basis of the universal banding pattern observed in various *Drosophila* tissues.

Keywords: Polytene chromosomes, Bands and interbands, *Drosophila*, Genes, Promoters, Proteins of open chromatin, Origin recognition complexes, *P*-elements.

1. INTRODUCTION

1.1. Polytene Chromosomes: Banding Pattern

Polytene chromosomes develop from the chromosomes of diploid nuclei by successive duplication of each chromosomal element (chromatid) without their segregation. The newly formed chromatids remain associated lengthwise and together form a cable-like structure, referred to as polytene chromosomes. In *Drosophila melanogaster*, they are 70-110 times longer than typical metaphase chromosomes [1]. Extent of coiling of the DNA and its associated proteins varies along the linear axis of each chromatid, thereby leading to the variation in chromatin concentration and compaction. Regions with high DNA content are known as chromomeres. In every polytene chromosome, homologous chromomeres align exactly alongside each other and so they fuse to form a transverse band. Bands are separated from each other by interchromomeric fragments of chromosomes (interbands). Thus, the alternation of compacted and decompacted regions of chromosomes – bands and interbands – appears in polytene chromosomes as black and white transverse stripes. The band/interband pattern of polytene chromosomes is remarkably constant in different cell types.

Three major morphological classes of structures are found in polytene chromosomes: interbands as well as grey and black bands [1- 4], these display distinct degrees of condensation (ratio between the length of the stretched DNA molecule and the length of the chromosomal structure it forms), gene expression profiles, replication timing, protein composition and enrichment with genetic elements. Highly decondensed and early-replicating interbands display DNA condensation ratio of about 5-12 [5]. Many bands are moderately condensed as well (12-73), yet they still appear as grey bands under microscope. These structures also tend to replicate early. Finally, the black bands are formed by densely compacted late-replicating material with the reported degree of compactization ranging from 158 to 204 [5, 6], and so they appropriately appear black under the microscope (Fig. **1**). Notably, many of the big (up to 600kb) black bands belong to a class of sequences called intercalary heterochro-

*Address correspondence to this author at the Institute of Molecular and Cellular Biology of the Russian Academy of Sciences, Novosibirsk 630090, Russian Federation; Tel: (+7) 383 363-90-42; Fax: (+7) 383 363-90-78; E-mail: zhimulev@mcb.nsc.ru

1389-2029/18 $58.00+.00

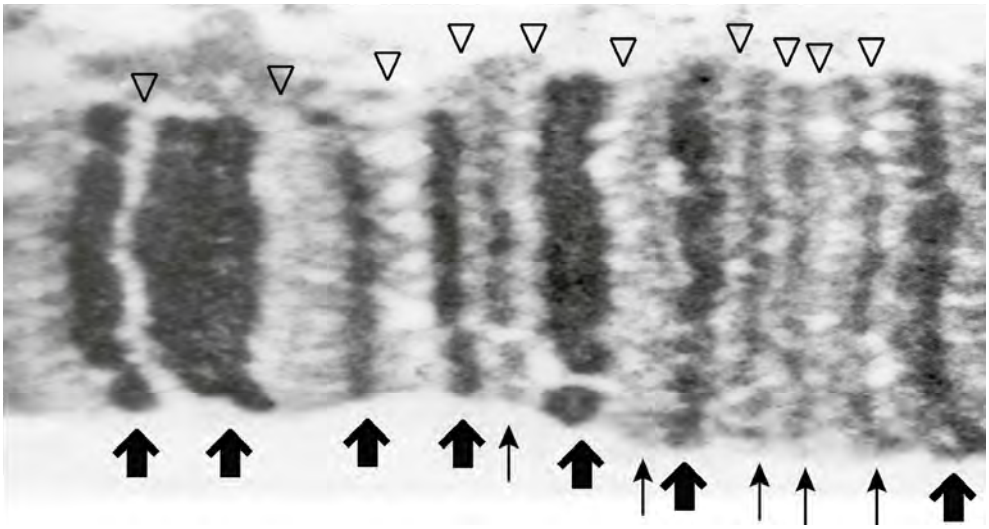

Fig. (1). Fragment of the polytene chromosome arm 3R showing compacted dark-staining bands (thick arrows), loose bands appearing grey (thin arrows), as well as interbands (arrowheads). The image is the courtesy of Dr. V.F. Semeshin.

matin (IH), as they demonstrate late replication, underreplication and ectopic pairing [7].

The exact number of bands present in polytene chromosomes has been debated in the literature, and conflicting data have been reported. The problem is that on the one hand, the seminal study by C. Bridges provided exquisitely fine and accurate drawings of poorly visible grey bands, whereas large black bands were over-fixed and appeared as rounded capsules with two walls. These doublet bands were artifacts indeed, but were nevertheless considered and drawn as separate bands, thereby two bands are present on the maps instead of just one. There are 5059 bands in the genome, of which 1207 account for doublets, really being singlets. Therefore, the total number of real bands (and hence interbands) is 5059-1207 = 3852. Given that very similar figures (about 3500) were found for the polytene chromosomes of many other dipteran species (using adequate fixation procedures and electron microscopy) and that the same number appears on the original maps by C. Bridges [3], we take this as the final number of bands in *Drosophila melanogaster* polytene chromosomes. Taking into account that doublets are formed by black bands, the approximate number of black bands is 1200, the number of grey bands is about 3500-1200=2400.

To get insight into the molecular and genetic organization of morphological elements in polytene chromosomes, cytology map must be compared with genetic and epigenetic maps obtained *via* genome-wide data of binding profiles of chromosomal proteins and histone modifications obtained in B. van Steensel laboratory and in frames of modEncode project [8, 9]. Clearly, this is nearly impossible to do in the absence of information of the positions of cytologically visible structures on the molecular map. Mapping interbands on the physical map is quite a challenging task due to their small size (0.04 - 0.14 micrometers) [5].

Our group took advantage of an approach that allows to obtain exactly this type of data by tagging interband material with P-element insertions (details in [3]). This permitted to get mapping data for 32 interbands. Upon closer inspection, it turned out that interbands share a number of common features. These include localization of TSSes of house-keeping genes, pronounced RNA polymerase II binding, low nucleosome density, histone H1 dips, broad promoters, DNAseI hypersensitive sites (DHS), enrichment with ORC components, interband-specific proteins CHRIZ, WDS, BEAF, nucleosome remodelers ISWI and NURF, and histone H3K4me3 mark specific for promoters of active genes [3]. Most important here is Chriz/CHROMATOR protein, discovered in laboratories of K.M. and J. Johansens [10] and H. Saumweber [11] which is cytologically located in every interband [12] and can serve as diagnostic instrument for mapping interbands.

2. CHROMATIN DOMAINS IN INTERPHASE CHROMOSOMES

In order to identify interband regions genome-wide, we selected a reference sent of 12 interband-specific and interband-enriched proteins. Localization data for these and other modEncode dataset proteins were fed into the custom-written Hidden Markov Model that partitioned the *Drosophila* genome into four color-coded basic chromatin types [3]. This model produces genome-wide localization data for interband state and three alternative states, so it allows for the first time to match the structures of polytene chromosomes and distinct chromatin types. To avoid possible confusion with similarly "colored" chromatin states and types reported by Filion *et al*. [8] and Kharchenko *et al.* [9], we chose to rename our four chromatin types as a gemstone palette: aquamarine, lazurite, malachite and ruby [10].

This mini-review is devoted to the analysis of modern data concerning molecular and genetic organization of specific polytene chromosome structures. As a result we hope to obtain general scheme describing functional sense of banding pattern.

Aquamarine-domains (formerly **cyan** chromatin [3]) constitute about 13% of the genome total. Our bioinformatic pipeline identifies about 5700 aquamarine domains in the genome [3], of which about 3500 display the features that

are typical for interbands (TSSes, Chriz and WDS binding, *etc*) (Fig. **2**). The remaining 2400 aquamarine domains correspond to the chromatin that has many features of open chromatin, and so these are recovered by the model, however they do not contain TSSes and location of interband-specific protein Chriz.

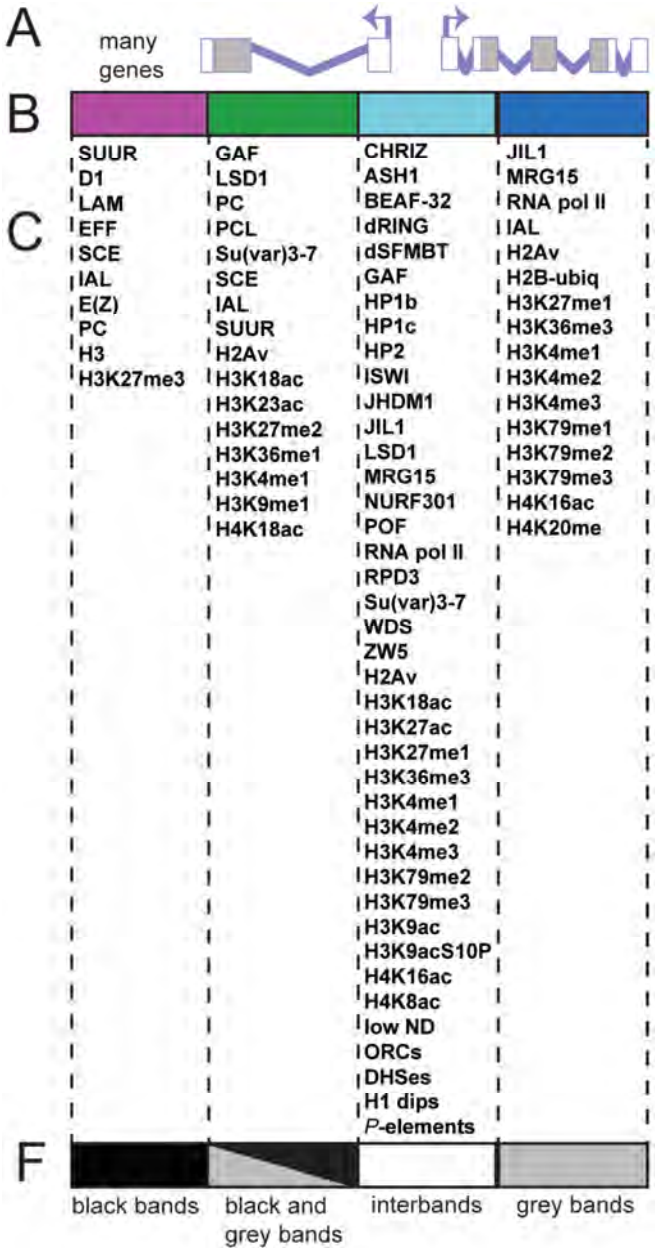

Fig. (2). Proteins, histone modifications and genomic elements that are stably present across the four chromatin types in S2, BG3 and Cl.8 cell lines.

A - Gene structure: exons and introns

B - Four states of chromatin domains, left to right: ruby, malachite, aquamarine, and lazurite

C - Proteins, histone modifications and genomic features enriched in the chromatin types

D - Types of chromosomal structures (grey and black bands, interbands) (according to [14] with modifications).

Localization of paused RNA polymerase II in these domains may support the idea that they are involved in transcription initiation, as expression in higher eukaryotes is controlled by an RNA polymerase stalling step early in elongation [15, 16]. Consistently, TSS+ aquamarine domains are particularly enriched for short RNAs derived from stalled RNA polymerase II in *Drosophila* cells [15] (Fig. **3**).

Several proteins and histone modifications implicated in gene silencing turned out to be significantly underrepresented in the aquamarine chromatin. Comparison of protein localization data for three cell lines (S2, BG3 and Cl.8) was indicative of high degree of similarity in protein and histone modification profiles between these cells [14] (Fig. **2**). Notably, the differences due to distinct origin of these cell lines (S2 is an embryo-derived cell line, BG3 is of neural origin, and Cl.8 was established from larval wing discs) were fairly small.

Lazurite chromatin (formerly, **blue** chromatin type [3]). This chromatin type accounts for 17% of the genome. Lazurite chromatin is associated with transcription-related histone modifications: H2B-ubiq, H2Av, H3K27me1, H3K4me1/2, and H3K36me3 (Fig. **2**). The latter histone modification is an established mark associated with elongating RNA polII and it is predominantly found in gene exons. This chromatin is poor in silent chromatin marks. There is significant enrichment of lazurite domains with JIL-1 and MRG15, both of which bind methylated H3K36 and H3K4 and participate in the maintenance of decompacted state of chromatin and regulate gene transcription (see [14] for references). This chromatin type is also moderately enriched in histone demethylase JMJD2A/KDM4A, which was reported to interact with HP1a and control the methylation status of H3K36.

Ruby chromatin (referred to as **magenta** chromatin [3]). As much as 48% of the genome falls into this chromatin type. Ruby chromatin is depleted for most of the proteins and histone modifications characteristic for active chromatin (Fig. **2**). Components of inactive chromatin E(Z), HP4, Su(var)3-9, PC, and PCL show moderate enrichment. Ruby chromatin is slightly enriched in histone H3. Histone marks associated with decondensed and active chromatin, namely H3K9ac, H3K27ac, H3K4me1/2/3, H3K4me3 and H4K16ac, display the most pronounced depletion within ruby domains. Analysis of DamID datasets indicates that in Kc cells, ruby chromatin is specifically enriched in ubiquitin ligase Effete (EFF) and LAM, and it is moderately enriched in SUUR and D1 proteins (for more details and references see [14]).

Malachite domains (former **green** chromatin [3]). This chromatin type constitutes 22% of the genome total. Malachite chromatin shows binding of TopoII, histone H3K4 demethylase LSD1, transcription regulator PC as well as Su(var)3-7, which shows genetic interaction with JIL-1. Malachite chromatin shows about 4-fold enrichment with histone marks H3K36me1 and H3K27me2. According to the DamID datasets, malachite chromatin appears to be associated with the prominent components of inactive chromatin, SUUR and D1, in Kc cells (Fig. **2**) (more details and references are provided [14]).

Thus, our expanded analysis confirmed the 4-state model: aquamarine and lazurite are active chromatin types;

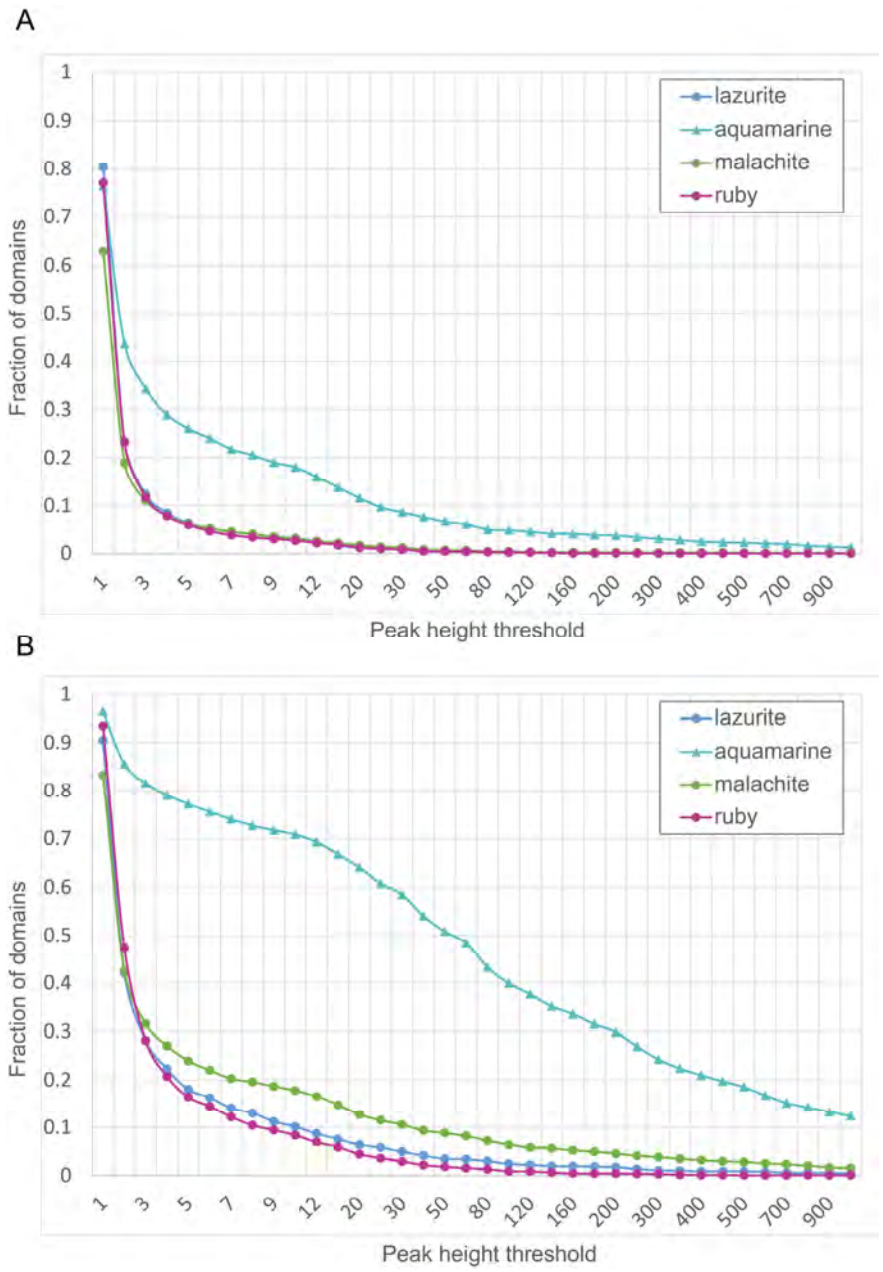

Fig. (3). GRO-Seq signal in four chromatin types of *Drosophila*
A - chromatin domains devoid of TSSes;
B - TSS-containing chromatin domains.
X-axis - numbers of 5'-forward short non-polyadenylated transcripts produced by the stalled RNA Pol II (data for 5' reverse, 3' reverse and 3' forward short RNA are identical and not shown) [15].
Y-axis - fraction of aquamarine, lazurite, malachite, and ruby chromatin domains.

ruby is inactive chromatin type, whereas malachite-chromatin is intermediate in terms of gene activity [3].

When comparing our chromatin painting data with earlier chromatin annotation projects (Table **1**), aquamarine type showed significant overlap with RED and YELLOW chromatin types [8], as well as with active chromatin states: promoter/TSS-enriched (state 1, red) and enhancer-enriched (state 3, brown) [9]. Lazurite chromatin in turn matched transcriptionally active YELLOW chromatin type [8] as well as state 2 (purple) and state 5 (active genes on the X chromosomes, green) [9].

In our analysis, no particular functions could be assigned to malachite domains [3]. Yet we observe partial overlap between malachite chromatin and silencing or repressed chromatin types [8] (Table **1**) or enhancers, introns of active genes, intercalary heterochromatin and inactive gene spacers [9]. Finally, ruby chromatin type clearly corresponds to BLUE and BLACK chromatin types [8] and inactive intergenic chromatin (light grey) or intercalary heterochromatin [9]. To summarize, all three studies converge in that they identify chromatin types and states that are broadly quite similar. However, our four color-coded model gives an

Table 1. Comparison of four chromatin types with Filion *et al.*, Kharchenko *et al.* and Milon *et al.* data.

Types of Chromatin:		**The Intersection of Four Chromatin Types with Five Chromatin Types from Filion *et al.* [6], nine chromatin types from Kharchenko *et al.* [8] and Milon *et al.* [12] (% of domain number):**			
From Filion *et al.* (Kc cell line) [6]:		**aquamarine**	**lazurite**	**malachite**	**ruby**
RED (Active)		37	5	15	1
YELLOW (Active, H3K36me3)		50	66	7	0
BLUE (PcG-silencing)		7	6	35	21
GREEN (HP1-silencing)		2	12	1	1
BLACK (Repressive)		4	11	42	77
From Kharchenko *et al.* (S2 and BG3 cell lines) [8]:		**aquamarine**	**lazurite**	**malachite**	**ruby**
State 1 (red) **S2**	(promoter/TSS)	48	13	0	0
State 1 (red) **BG3**		44	10	0	0
State 2 (purple) **S2**	(transcription)	5	60	9	1
State 2 (purple) **BG3**		5	61	7	0
State 3 (brown) **S2**	(enhancer)	32	3	14	0
State 3 (brown) **BG3**		33	4	20	2
State 4 (coral) **S2**	(active intron)	4	1	24	11
State 4 (coral) **BG3**		5	1	24	14
State 5 (green) **S2**	(active gene on X)	3	19	8	1
State 5 (green) **BG3**		3	20	6	1
State 6 (dark grey) **S2**	(PcG-repression)	1	0	6	10
State 6 (dark grey) **BG3**		1	0	5	10
State 7 (dark blue) **S2**	(pericentric heterochromatin)	2	3	3	4
State 7 (dark blue) **BG3**		2	2	2	2
State 8 (light blue) **S2**	(intercalary heterochromatin)	0	0	2	4
State 8 (light blue **BG3**		1	0	10	29
State 9 (light grey) **S2**	(inactive intergenic)	5	2	32	69
State 9 (light grey) **BG3**		6	1	25	42
The degree of compaction of chromatin from Milon *et al.*, 2014 (S2 cell lines) [12]:		**aquamarine**	**lazurite**	**malachite**	**ruby**
+1	Open	84	44	30	4
0	Neutral	62	38	87	68
-1	Closed	2	2	28	89

advantage in possibility to map interband-specific chromatin state, *i.e.* gives an opportunity to map interbands.

Using high-throughput analysis for general chromatin sensitivity to DNase I, contiguous domains of open and closed chromatin were identified and the chromatin was partitioned into three major compactness classes: open (+1), neutral (0), and closed (-1) [17]. Aquamarine and lazurite chromatin essentially matched open and neutral chromatin classes, malachite was largely composed of the

neutral class, and ruby corresponded to closed or neutral classes (Table **1**).

3. CORRESPONDENCE BETWEEN FOUR CHROMATIN TYPES AND STRUCTURAL PARTS OF THE GENES

To address the question of whether the four chromatin types may correspond to distinct parts of the genes, such as TSS, exons, introns, *etc*, as well as intergenic intervals, we mapped the borders of chromatin types within these genetic features. By comparing their positions with those of 13237 protein-coding genes of *Drosophila* and all 28013 annotations marked as 'mRNA', we found that different chromatin types are non-randomly distributed relatively to the structural parts of the genes. In particular, 58% of aquamarine-chromatin domains fragments encompass TSSes while the percent overlap of TSSes with the other three chromatin types is significantly lower. Lazurite chromatin largely corresponds (82%) to transcribed portions of the genes, *i.e.* to GENE class (Fig. **4**). About half of malachite and ruby chromatin sequences belong to introns and intergenic regions. Much like lazurite chromatin, malachite chromatin is rarely found at or near TSSes. Ruby chromatin is moderately depleted for TSS-class sequences and similarly to malachite chromatin, it rarely maps to introns, intergenic regions or gene bodies. This may be due to the fact that ruby chromatin typically spans large genomic regions, and so it encompasses many entire genes, not just gene elements.

4. MUTUAL POSITIONING OF THE FOUR CHROMATIN TYPES IN THE GENOME

Taking into account that aquamarine and lazurite chromatin types tend to correlate with TSS- and GENE-class sequences, respectively (see above), these two chromatin types were expected to locate side-by-side, a pattern that was supposed to depend on the direction of transcription. Therefore, we examined how the chromatin types are positioned relatively one another. Somewhat surprisingly, we observed that lazurite and aquamarine-chromatin domains never bordered ruby-chromatin, which in turn was found to exclusively contact malachite-chromatin.

Next, we proceeded to analyze whether transitions between chromatin types are in any way related to the gene structure. We calculated the number of transitions for each chromatin type pair per 1000 bp of the total length of each structural part of all the transcripts. The following elements were considered: 5'UTR and 3'UTR exons, 1st, 2nd, 3rd, and the rest of the coding exons, all introns, and intergenic spacers. Transcription direction was accounted for as follows: all transition points for each pair of chromatin types (for instance, aquamarine-lazurite, lazurite-aquamarine) were mapped chromosome (genome)-wide. The statistical significance of differences was estimated by Fischer's *t*-test for angular (arcsine square root) transformed proportions [18].

Then, the coordinates of these transition points were compared to the borders of the structural parts of genes and so four transition patterns per chromatin type pair were formed (Fig. **5**). We observed that aquamarine-lazurite transition points tend to map to the first coding exons of the genes: 2nd (0.37 borders/kb, p< 1E-745), 1st (0.21 borders/kb, p< 1E-582), 3rd (0.14 borders/kb, p< 1E-134). Notably, opposite transitions (lazurite-to-aquamarine) are significantly less frequent (0.007 borders/kb, 2nd exon). The frequencies of the rest of transitions between chromatin types were below the significance levels (Fig. **5**).

Thus, we demonstrated that transition points from aquamarine- into lazurite-chromatin types are predominantly found within gene bodies, specifically within the first two protein-coding exons. Notably, of all the aquamarine-to-lazurite and lazurite-to-aquamarine borders in the genome, 52.1% fall into a group where transition pattern matches the direction of transcription: 5'- aquamarine - lazurite -3', and where the border maps to the coding exons. In other words, aquamarine chromatin tends to locate upstream of the lazurite, and in most cases these two chromatin types appear coupled within the same gene. Other combinations of transitions between the chromatin types did not display significant association with transcription direction (Fig. **5**). When this analysis was applied to 9 chromatin states identified from the patterns of histone modificiations, a similar trend was visible: TSSes (red state) are invariably upstream of transcription-associated purple state (in autosomes) or green state (on the male X) (Fig. **S8** in [9]).

5. GENETIC ORGANIZATION OF BANDS AND INTERBANDS

As was noted above, all the 32 cytology-mapped interbands encompassed TSSes and aquamarine chromatin. Across the genome, about 3350 TSS-containing aquamarine domains were found, which closely matches the estimates of the number of interbands (about 3500, see above). The remaining 2400 aquamarine domains lack TSSes as well as many other features associated with interbands. Thus, while every interband is represented by aquamarine chromatin, the opposite is not always true. Interbands correspond to permanently decondensed regions of chromosomes, which provides a morphological support to the observation that interbands host TSSes of house-keeping genes [3].

Interbands are particularly rich in ORCs (91% of ORCs are found in aquamarine chromatin) [3]. Therefore interbands appear to be the structures where two fundamental processes-transcription and replication – initiate.

Lazurite chromatin domains are typically found adjacent to and downstream of acquamarine domains (Fig. **5**). In the context of polytene chromosomes, interbands are typically bordered by grey bands, which argue for the idea that this class of bands hosts coding parts of genes [3]. Thus, when we compare the mapping results obtained using different approaches, *i.e.* localization of RED and GREEN chromatin [8], aquamarine and lazurite chromatin (Fig. **6**) *vs*. bands and interands found in polytene chromosomes [5], the correspondence between the banding pattern and chromatin types becomes obvious. However, there are some cases of exclusions: in the interbands 10A1-2/10A3 and 10AB1-2/10B3 short genes are located which are not connected with neighboring bands (Fig. **6** in [3]). In the interband 61C7/61C8 by method of high resolution *in situ* hybridization there was found several active genes and this region "can be considered as an open chromatin domain" [13].

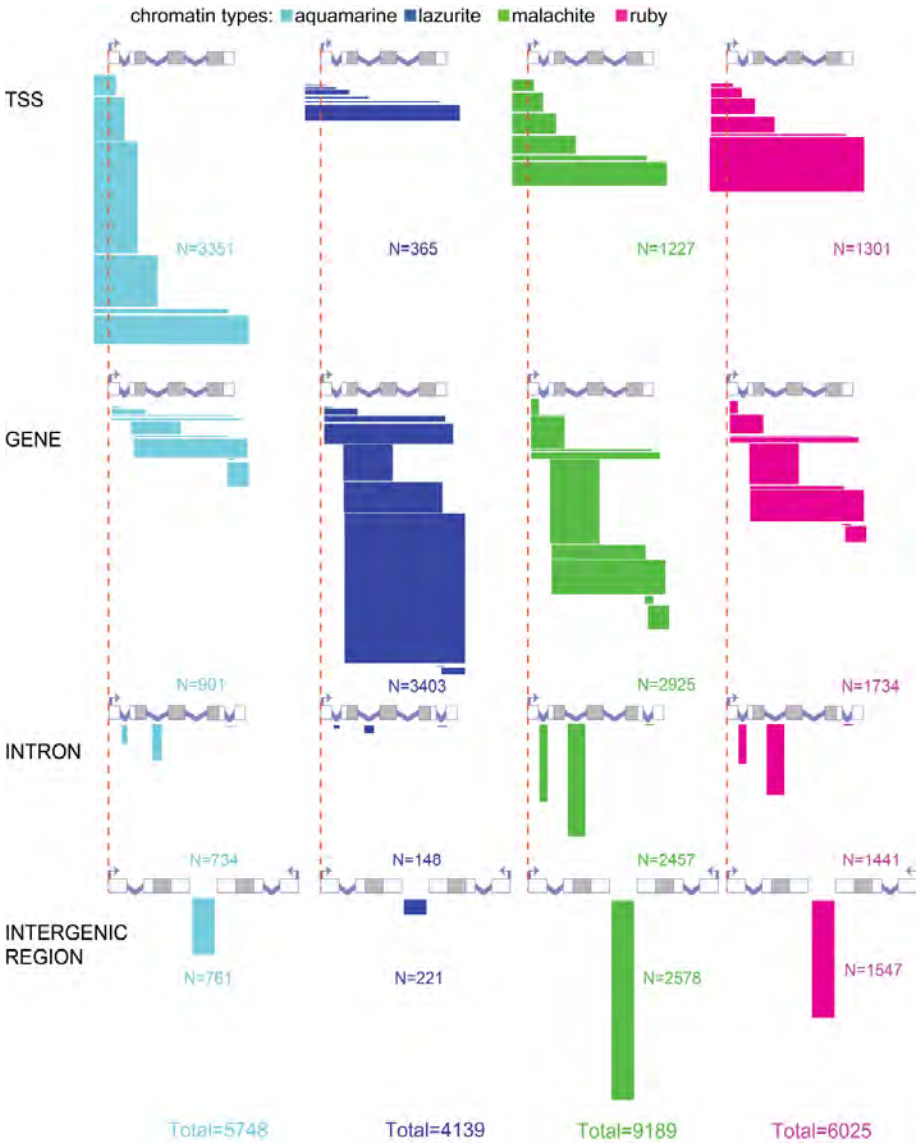

Fig. (4). Detailed classification of relative positioning of aquamarine, lazurite, malachite and ruby chromatin domains and gene structure in the four chromatin types. Bent arrows and red vertical dashed lines indicate the positions of TSSes. Grey boxes represent coding parts of exons and white boxes correspond to 5' and 3' UTRs. Introns are shown as broken lines. Horizontal bars depict different possible overlaps between chromatin domains and genes for all localization classes: TSS, GENE, INTRON and INTERGENIC REGION. The width of each bar reflects the number of each localization subclass in each chromatin type (according to [14]). (*For interpretation of the references to color in this figure legend, the reader is referred to the web version of this paper.*)

Finally, ruby-chromatin, which usually corresponds to the highly compacted late-replicating black bands in polytene chromosomes including those classified as intercalary heterochromatin. Originally described almost 80 years ago [19], IH regions stand out as a particular type of polytene chromosome bands that form chromosome breaks and chromosome fibers when ectopically paired with other IH regions and regions of pericentric heterochromatin. Subsequent analysis of IH established these regions as replicating late in the cell cycle [7] and undergoing underreplication – the consequence of extremely late replication in the cell cycle. IH bands are made of the chromatin that is repressed both in salivary glands and in cell lines [20]; these regions display low gene density [21] and comprise clusters of functionally not related genes with narrow tissue-specific expression [7, 20-22].

6. BANDING PATTERN AND TOPOLOGICALLY ASSOCIATING DOMAINS

Besides epigenetic partitioning, the *Drosophila* genome has been reported to be organized, into structural domains – the chromatin regions that show significant self-interactions.

(Topologically Associating Domains - TADs, or physical domains). Top-domains have been identified based on their frequent ligation to each other upon chromatin cross-linking ([6, 23-26] and references therein). Boundaries of the top-domains, much as interbands, are enriched for insulator proteins CTCF, BEAF-32, CP190, and CHRIZ. This in turn pointed to an intriguing possibility that top-domains and boundaries of top-domains can be visualized as a banding pattern of polytene chromosomes [23]. Appropriately, we

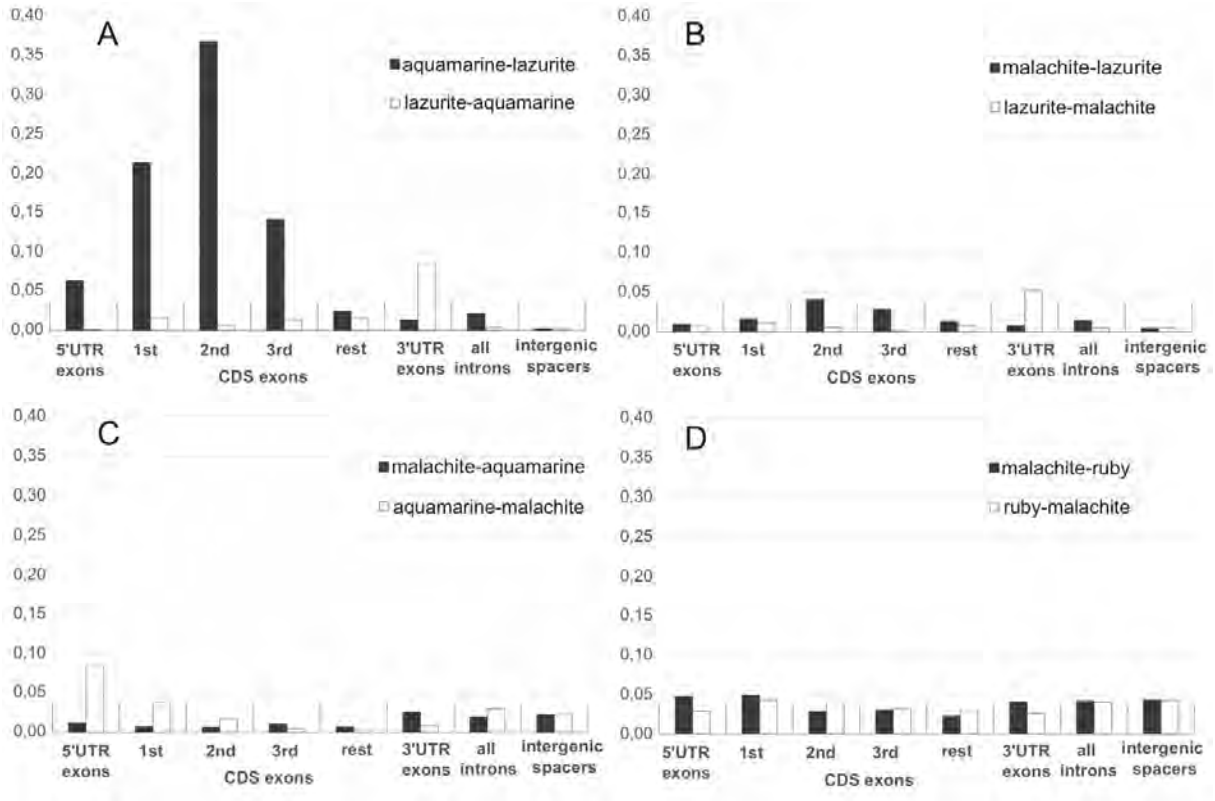

Fig. (5). Localization frequencies for all pairwise combinations of the four chromatin types. All transitions were counted in a sense direction of transcription. X axis shows the structural parts considered in the analysis: 5'UTR and 3'UTR exons, 1st, 2nd, 3rd and the rest of the coding exons, all introns, and intergenic spacers. Y axis shows the number of transitions between chromatin types normalized by the length of an appropriate structural part.

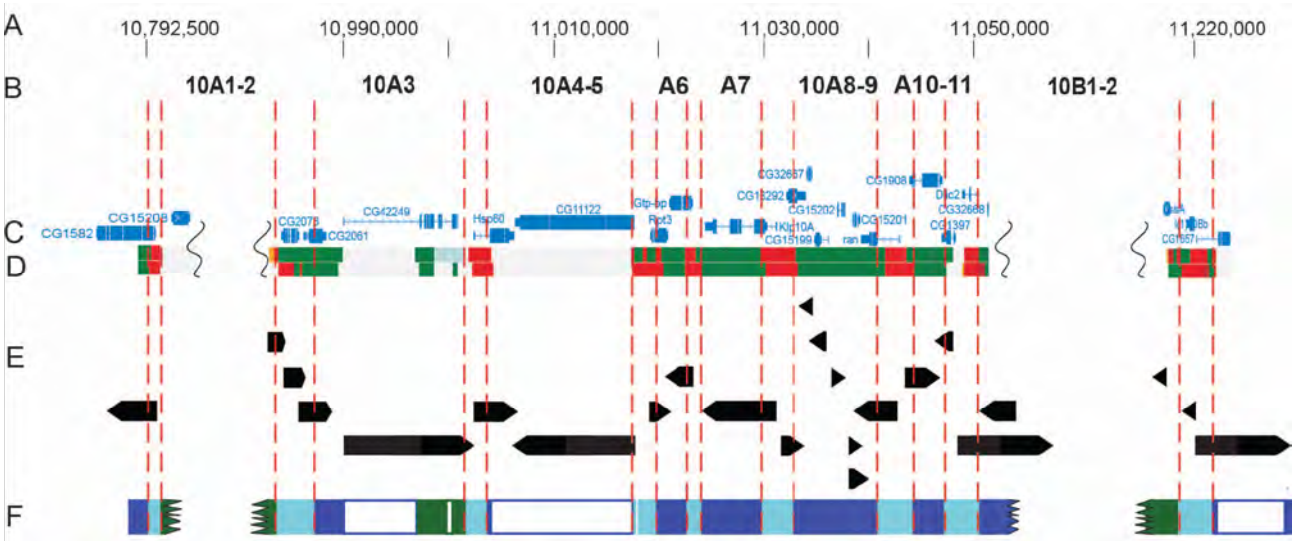

Fig. (6). Comparison of the mapping data for bands and interbands in the region 10A1-2 - 10B1-2 of the polytene X chromosome and chromatin states and types, as defined by Kharchenko *et al*. (**C**, **D**) [9, 5] and Zhimulev *et al*. (**E**, **F**) [3].

A - Genomic coordinates (FlyBase r.5.50)
B - Bands (from [6, 5])
C - Gene map (FlyBase r.5.50)
D - Positions of promoter/TSS domains (red) and X-chromosomal active chromatin state (green) according to Kharchenko [9].
E - Gene positions according to [3]
F - Positions of aquamarine and lazurite chromatin domains [4] and colocalization with interbands and grey bands. The borders of bands/interbands are designated by red dashed lines. White boxes indicate absence of data from the modEncode datasets. (*For interpretation of the references to color in this figure legend, the reader is referred to the web version of this paper.*)

observed that a group of polytene chromosome bands corresponded to top domains [3]. Recent genome-wide analysis of TAD localization in *Drosophila* salivary gland cells argued in favor of this idea [6], and so positions of TADs could be compared to the localization of molecularly mapped bands. The authors demonstrated that HiC approach correctly predicts the positions of bands and interbands, with notable correspondence between TADs and polytene chromosome bands and absence thereof in puffs. These results were further supported by FISH mapping data for the probes from TAD centers and borders to bands and interbands, respectively [3, 6]. Before as it was shown that of intercalary heterochromatin bands are evolutionary conservative [27] and these bands are TAD domains, we may conclude that TADs are conservative not only in different tissues, but in evolution as well.

7. INTERPHASE CHROMOSOMES FROM *DROSOPHILA* CELL LINES AND SALIVARY GLANDS DEMONSTRATE IDENTICAL ORGANIZATION

All the protein profiling data generated by the modEncode consortium illustrate chromatin organization in interphase chromosomes of *Drosophila* cell lines (mitotically active, nearly diploid cells), in contrast chromosome banding is a feature only observable in polytene chromosomes. Whereas the long-held consensus in the field was that these two types of chromosomes were largely identical, until recently no experimental proof for this idea has been presented.

The identity and uniformity of interphase chromosome organization across different cell types are supported by the data on localization of DNA probes in these chromosomes (Table **2**). First of all, this stems from the identical positions of interbands in both types of chromosomes, which has been confirmed by co-localization of an interband-specific protein Chriz and the DNA probe of the interband material [5]. The second evidence comes from reciprocal EM localization of transposon insertions, when interbands whose positions were defined based on the aquamarine chromatin coordinates (derived from the cell line datasets) were shown to bear insertions of transposons in the appropriate interbands (Table **2**).

The largest black bands, IH bands, were mapped on the physical map based on the reduced copy number of their DNA in polytene chromosomes, which is a result of their late replication and underreplication [21, 22, 28]. Mapping data for 60 IH bands could be combined with the data on positions of the flanking interbands and so their molecular features could be compared between cell lines and salivary glands. This analysis supports the idea that IH regions are identically organized across various cell types [7], which is also consistent with the stability of TADs in polytene chromosomes and the chromosomes from cell lines [6].

Most interesting is mapping the big band 10A1-2 with very appropriate markers, *v* and *sev* genes on both edges of the late replicated band in the polytene chromosomes and the positioning these genes on the edges of late replicated ruby domain in the cell lines chromosome (Table **2**).

Thus, we conclude that the pattern of alternating chromatin domains having distinct condensation status is detectable in polytene chromosomes as banding pattern; furthermore it is also inherent to the interphase chromosomes of cell lines. Structural elements (two types of bands and interbands) in these chromosome types appear conserved and display very similar borders and sets of associated proteins.

The conclusion about similarity of chromosome organization in polytene and diploid cells does not mean complete identity of the genome in different cell types; it concerns only euchromatic parts of chromosomes, because it is known that pericentromeric heterochromatin is underreplicated in polytene chromosomes and almost does not contain both genes and bands.

Thus, contrary to beliefs, polytene chromosomes are in fact not too exotic entities; they share the same universal organization principle with the interphase chromosomes from diploid cells [29].

CONCLUSION

The polytene chromosome banding was described for the first time as long ago as in 1934 - 1935 by T. Painter, N. Kolltzoff and C. Bridges [1-3], namely they started the discussion on genetic organization of bands and interbands.

Functional organization of polytene chromosomes was first discussed in the seminal works of W. Beermann who proposed that local chromatin decondensation observed during puff formation which is linked to gene activation. This idea later received experimental support in studies using *Drosophila* and *Chironomus* polytene chromosomes by H. Berendes and M. Ashburner ([30-32] and references therein). These studies have paved the way to the comprehensive analyses of genetic composition of bands, puffs and interbands.

The new principle of gene organization in polytene chromosomes was suggested by F. Crick and J. Paul in 1971 - 1972 [33, 34], they proposed that a gene occupies two chromosome structures - bands and interbands: regulatory elements are in a band, while structural part is in neighboring interband (F. Crick) and *vice versa*, regulatory gene part is located in interband, and structural part in the band (J. Paul). The last hypothesis got very good support in modern research discussed in this mini-review.

Especially acute discussion about band organization started in 1972, when in laboratory of B. Judd [35] was shown numerical correspondence between essential genes and thin grey bands in a short chromosome region. Subsequently in many other regions such numerical 1:1 correspondence was found after "saturation" the regions with lethal mutations – the method giving possibility to find essential for surviving genes [36] and one may judge that in *Drosophila* genome there are about 3,500 genes – one per a band.

At first glance after *Drosophila* genome sequencing this hypothesis should die because the number of genes in the whole genome (more than 13,000) completely overwhelms the band number. However, if to admit that the housekeeping genes could be "essential" it is very easy to propose that in regions of thin grey bands (Judd's region) the number of genes really corresponds to the number of bands/interbands. The rest of genes are located in the ruby bands where numerous genes are located. Analysis of other previously "saturated" regions could give much interesting data.

Table 2. Correspondence in localization of chromosome structures in diploid and polytene cells.

Coordinates (FlyBase R. 5.50)	Interphase Chromosomes of Cell Lines*	Polytene Chromosomes*
chrX:10792601-10793800	Aquamarine chromatin domain, the distal border of ruby chromatin domain	Interband 9F13/10A1-2, the distal border of band 10A1-2
	Localization of protein CHRIZ by ChIP-Chip	Immunofluorescence localization of protein CHRIZ
	Localization of NSL complex proteins by ChIP-chip and ChIP-seq	Localization of NSL complex proteins by ChIP-seq
		Localization of FISH probe on the distal border of ruby domain chrX:10794864-10795492
chrX:10793801-10983600	Ruby chromatin domain	Black band 10A1-2
	Localization of vermilion and sevenless genes	Localization of vermilion and sevenless genes
	Low gene density	Low gene density
	Late replication	Late replication
	Localization of protein SUUR by ChIP-Chip	Immunofluorescence localization of protein SUUR
chrX:10983601-10987200	Aquamarine chromatin domain, proximal border of ruby chromatin domain	Interband 10A1-2/10A3, the proximal border of band 10A1-2
	Localization of protein CHRIZ by ChIP-Chip	Immunofluorescence localization of protein CHRIZ
	Transposon w* P{EP}G400 insertions	EM mapping of transposon w* P{EP}G400 insertions
		Localization of FISH probe on the proximal border of ruby domain chrX:10983459-10983987
chrX:10987201-11001600	Lazurite and malachite chromatin domains	Grey band 10A3
chrX:11001601-11003600	Aquamarine chromatin domain	Interband 10A3/10A4-5
	Localization of protein ORC2 by ChIP-seq	Localization of protein ORC2 by ChIP-seq
	Localization of NSL complex proteins by ChIP-chip and ChIP-seq	Localization of NSL complex proteins by ChIP-seq
	Transposon $y^{1}w^{67c23}P\{EPgy2\}Hsp60^{EY01572}$ insertions	EM mapping of transposon $y^{1}w^{67c23}P\{EPgy2\}Hsp60^{EY01572}$ insertions
chrX:11003601-1101760	Lazurite chromatin domain	Grey band 10A4-5
chrX:11017601-11019800	Aquamarine chromatin domain	Interband 10A4-5/10A6
	Localization of protein ORC2 by ChIP-seq	Localization of protein ORC2 by ChIP-seq
	Localization of NSL complex proteins by ChIP-chip and ChIP-seq	Localization of NSL complex proteins by ChIP-seq
chrX:11019801-11022600	Lazurite chromatin domain	Grey band 10A6
chrX:11022601-11024000	Aquamarine chromatin domain	Interband 10A6/10A7
chrX:11024001-11029800	Lazurite chromatin domain	Grey band 10A7
chrX:11029801-11032800	Aquamarine chromatin domain	Interband 10A7/10A8-9
	Localization of protein ORC2 by ChIP-seq	Localization of protein ORC2 by ChIP-seq
	Localization of NSL complex proteins by ChIP-chip and ChIP-seq	Localization of NSL complex proteins by ChIP-seq
	Transposon $y^{1}P\{EPgy2\}EY09320w^{67c23}$ insertions	EM mapping of transposon $y^{1}P\{EPgy2\}EY09320w^{67c23}$ insertions

(Table 2) contd….

Coordinates (FlyBase R. 5.50)	Interphase Chromosomes of Cell Lines*	Polytene Chromosomes*
chrX:11032801-11040800	Lazurite chromatin domain	Grey band 10A8-9
chrX:11040801-11044200	Aquamarine chromatin domain	Interband 10A8-9/10A10-11
	Localization of protein ORC2 by ChIP-seq	Localization of protein ORC2 by ChIP-seq
	Localization of NSL complex proteins by ChIP-chip and ChIP-seq	Localization of NSL complex proteins by ChIP-seq
chrX:11044201-11047200	Lazurite chromatin domain	Grey band 10A10-11
chrX:11040801-11044200	Aquamarine chromatin domain	Interband 10A8-9/10A10-11
	Localization of protein CHRIZ by ChIP-Chip	Immunofluorescence localization of protein CHRIZ
	Localization of protein ORC2 by ChIP-seq	Localization of protein ORC2 by ChIP-seq
		Localization of FISH probe on the distal border of ruby domain chrX:11050926-11051486
chrX:11050801-11217800	Ruby chromatin domain	Black band 10B1-2
	Low gene density	Low gene density
	Late replication	Late replication
	Localization of protein SUUR by ChIP-Chip	Immunofluorescence localization of protein SUUR
chrX:11217801-11221000	Aquamarine chromatin domain	Interband 10B1-2/10B3
	Localization of protein CHRIZ by ChIP-Chip	Immunofluorescence localization of protein CHRIZ
	Localization of protein ORC2 by ChIP-seq	Localization of protein ORC2 by ChIP-seq
	Localization of NSL complex proteins by ChIP-chip and ChIP-seq	Localization of NSL complex proteins by ChIP-seq
		Localization of FISH probe on the proximal border of ruby domain chrX:11218703-11219201
Topologically Associating Domains (TADs) are conserved between polytene and diploid cells*		

*Data and all references are in [4-7].

Completion of the *Drosophila* genome sequencing combined with the advent of approaches to map chromatin states genome-wide as well as with novel tools to map bands and interbands, have made it possible to perform molecular and genetic analyses of these structures in polytene chromosomes. Here, we highlight the major results of these efforts.

The striking similarities between organization of polytene chromosomes and chromosomes from cell lines justify the former as a robust model of interphase chromosomes and so their morphology may be considered as a portrait of the genome, - a portrait showing how it is organized and how it functions.

Interbands function as the hubs where initiation of both transcription and replication occurs. Molecularly, the interbands correspond to the 5'-regulatory regions of housekeeping genes. The coding regions of these genes typically map to adjacent loosely condensed (grey) bands. Strongly compacted (black) bands of IH contain clusters of repressed tissue- and stage-specific genes. Thus, the banding pattern found across different cell types is based on the invariably active chromatin of interbands, moderate decompaction of grey bands and repressed state of IH bands [37].

CONSENT FOR PUBLICATION

Not applicable.

CONFLICT OF INTEREST

The authors declare no conflict of interest, financial or otherwise.

ACKNOWLEDGEMENTS

This work was supported by the grant 14-14-00934 from the Russian Science Foundation (RSF) and the bioinformatics analysis was supported by the ICG SB RAS and MCB SB RAS budget projects 0310-2016-0005 and 0310-2016-0009, respectively. All four authors contributed to writing this manuscript.

REFERENCES

[1] Painter, T.S. Salivary chromosomes and the attack on the gene. *J. Hered.*, **1934**, *25*(12), 465-476. Available from: https://academic.oup.com/jhered/article-abstract/25/12/465/807076? redirected-From=fulltext

[2] Koltzoff, N.K. The structure of the chromosomes in the salivary glands of *Drosophila*. *Science*, **1934**, *80*(2075), 312-313. Available from: science.sciencemag.org/content/80/2075/312

[3] Bridges, C.B. Salivary chromosome maps with a key to the banding of the chromosomes of *Drosophila melanogaster*. *J. Hered.*, **1935**, *26*(2), 60-64.

[4] Zhimulev, I.F.; Zykova, T.Y.; Goncharov, F.P.; Khoroshko, V.A.; Demakova, O.V.; Semeshin, V.F.; Pokholkova, G.V.; Boldyreva, L.V.; Demidova, D.S.; Babenko, V.N.; Demakov, S.A.; Belyaeva, E.S. Genetic organization of polytene chromosome bands and interbands in *Drosophila melanogaster*. *PLoS One*, **2014**, *9*(7), e101631. Available from: journals.plos.org/plosone/article?id=10.1371/journal.pone.0101631

[5] Vatolina, T.Y.; Boldyreva, L.V.; Demakova, O.V.; Demakov, S.A.; Kokoza, E.B.; Semeshin, V.F.; Babenko, V.N.; Goncharov, F.P.; Belyaeva, E.S.; Zhimulev, I.F. Identical functional organization of nonpolytene and polytene chromosomes in *Drosophila melanogaster*. *PLoS One*, **2011**, *6*(10), e25960. Available from: journals.plos.org/plosone/article?id=10.1371/journal.pone.0025960

[6] Eagen, K.P.; Hartl, T.A.; Kornberg, R.D. Stable chromosome condensation revealed by chromosome conformation capture. *Cell*, **2015**, *163*(4), 934-946.

[7] Belyaeva, E.S.; Goncharov, F.P.; Demakova, OV.; Kolesnikova, T.D.; Boldyreva, L.V.; Semeshin, V.F.; Zhimulev, I.F. Late replication domains in polytene and nonpolytene cells of *Drosophila melanogaster*. *PloS One*, **2012**, *7*(1), e30035. Available from: journals.plos.org/plosone/article?id=10.1371/journal.pone.0030035

[8] Filion, G.J.; van Bemmel, J.G.; Braunschweig, U.; Talhout, W.; Kind, J.; Ward, L.D.; Brugman, W.; de Castro, I.J.; Kerkhoven, R.M.; Bussemaker, H.J.; van Steensel, B. Systematic protein location mapping reveals five principal chromatin types in *Drosophila* cells. *Cell,* **2010**, *143*(2), 212-224. Available from: science.sciencemag.org/content/330/6012/

[9] modENCODE Consortium. Identification of functional elements and regulatory circuits by *Drosophila* modENCODE. *Science,* **2010**, *330*(6012), 1787-1797. Available from: science.sciencemag.org/content/330/6012/

[10] Kharchenko, P.V.; Alekseyenko, A.A.; Schwartz, Y.B.; Minoda, A.; Riddle, N.C.; Ernst, J.; Sabo, P.J.; Larschan, E.; Gorchakov, A.A.; Gu, T.; Linder-Basso, D.; Plachetka, A.; Shanower, G.; Tolstorukov, M.Y.; Luquette, L.J.; Xi, R.; Jung, Y.L.; Park, R.W.; Bishop, E.P.; Canfield, T.K.; Sandstrom, R.; Thurman, R.E.; MacAlpine, D.M.; Stamatoyannopoulos, J.A.; Kellis, M.; Elgin, S.C.; Kuroda, M.I.; Pirrotta, V.; Karpen, G.H.; Park, P.J. Comprehensive analysis of the chromatin landscape in *Drosophila melanogaster*. *Nature,* **2011**, *471*(7339), 480-485. Available from: www.nature.com/nature/journal/v471/n7339/abs/nature09725.html

[11] Rath, U.; Wang, D.; Ding, Y.; Xu, Y.Z.; Qi, H.; Blacketer, M.J.; Girton, J.; Johansen, J.; Johansen, K.M. Chromator, a novel and essential chromodomain protein interacts directly with the putative spindle matrix protein skeletor. *J. Cell Biochem.,* **2004**, *93*(5),1033-1047.

[12] Eggert, H.; Gortchakov, A.A.; Saumweber H. Identification of the *Drosophila* interband-specific protein Z4 as a DNA binding zinc-finger protein determining chromosomal structure. *J. Cell Sci.,* **2004**, *117*(Pt18), 4253-4264.

[13] Gortchakov, A.A.; Eggert, H.; Gan, M.; Mattow, J.; Zhimulev, I.F.; Saumweber, H. Chriz, a chromodomain protein specific for the interbands of *Drosophila melanogaster* polytene chromosomes. *Chromosoma*, **2005**, *114*(1), 54-66.

[14] Zielke, T.; Glotov, A.; Saumweber, H. High-resolution *in situ* hybridization analysis on the chromosomal interval 61C7-61C8 of *Drosophila melanogaster* reveals interbands as open chromatin domains. *Chromosoma*, **2015**, *125*(3), 423-435.

[15] Boldyreva, L.V.; Goncharov, F.P.; Demakova, O.V.; Zykova, T.Y.; Levitsky, V.G.; Kolesnikov, N.N.; Pindyurin, A.V.; Semeshin, V.F.; Zhimulev, I.F. Protein and genetic composition of four basic epigenetic domains in cell line chromosomes of *Drosophila melanogaster*. *Curr. Genomics*, **2017**, *18*(2), 214-226.

[16] Nechaev, S.; Fargo, D.C.; dos Santos, G.; Liu, L.; Gao, Y.; Adelman, K. Global stalling of short RNAs reveals widespread promoter-proximal stalling and arrest of Pol II in *Drosophila*. *Science*, **2010**, *327*(5963), 335-338. Available from: science.sciencemag.org/content/327/5963/335

[17] Scruggs, B.S.; Gilchrist, D.A.; Nechaev, S.; Muse, G.W.; Burkholder, A.; Fargo, D.C.; Adelman, K. Bidirectional transcription arises from distinct hubs of transcription factor binding and active chromatin. *Mol. Cell*, **2015**, *58*(6), 1101-1112.

[18] Milon, B.; Sun, Y.; Chang, W.; Creasy, T.; Mahurkar, A.; Shetty, A.; Nurminsky, D.; Nurminskaya, M. Map of open and closed chromatin domains in *Drosophila* genome. *BMC Genomics*, **2014**, *15,* 988. Available from: https://bmcgenomics.biomedcentral.com/articles/10.1186/1471-2164-15-988

[19] Sokal, R.R.; James, R.F. *Biometry: The Principles and Practice of Statistics in Biological Research*. SERBIULA: (sistema Librum 2.0), **2013**.

[20] Kaufmann, B.P. Distribution of induced breaks along the X-chromosome of *Drosophila melanogaster*. *Proc. Natl. Acad. Sci. U.S.A.,* **1939**, *25*(11), 571-577.

[21] Sher, N.; Bell, G.W.; Li, S.; Nordman, J.; Eng, T.; Eaton, M.L.; Macalpine, D.M.; Orr-Weaver, T.L. Developmental control of gene copy number by repression of replication initiation and fork progression. *Genome Res*., **2012**, *22*(1), 64-75.

[22] Belyakin, S.N.; Christophides, G.K.; Alekseyenko, A.A.; Kriventseva, E.V.; Belyaeva, E.S.; Nanayev, R.A.; Makunin, I.V.; Kafatos, F.C.; Zhimulev, I.F. Genomic analysis of *Drosophila* chromosome underreplication reveals a link between replication control and transcriptional territories. *Proc. Natl. Acad. Sci. U.S.A.,* **2005**, *102*(23), 8269-8274.

[23] Yarosh, W.; Spradling A.C. Incomplete replication generates somatic DNA alterations within *Drosophila* polytene salivary gland cells. *Genes Dev.,* **2014**, *28*(16), 1840-1855.

[24] White, R. Packaging the fly genome: Domains and dynamics. *Brief Funct. Genomics,* **2012**, *11*(5), 347-355.

[25] Sexton, T.; Yaffe, E.; Kenigsberg, E.; Bantignies, F.; Leblanc, B.; Hoichman, M.; Parrinello, H.; Tanay, A.; Cavalli, G. Three-dimensional folding and functional organization principles of the *Drosophila* genome. *Cell*, **2012**, *148*(3), 458-472.

[26] Hou, C.; Li, L.; Zhaohui, S.; Qin, Z.S.; Corces, V.G. Gene density, transcription, and insulators contribute to the partition of the *Drosophila* genome into physical domains. *Mol. Cell*, **2012**, *48*(3), 471-484.

[27] Ulianov, S.V.; Khrameeva, E.E.; Gavrilov, A.A.; Flyamer, I.M.; Kos, P.; Mikhaleva, E.A.; Penin, A.A.; Logacheva, M.D.; Imakaev, M.V.; Chertovich, A.; Gelfand, M.S.; Shevelyov, Y.Y.; Razin, S.V. Active chromatin and transcription play a key role in chromosome partitioning into topologically associating domains. *Genome Res*., **2016**, *26*(1), 70-84.

[28] Andreyenkova, N.G.; Kolesnikova, T.D.; Makunin, I.V.; Pokholkova, G.V.; Boldyreva, L.V.; Zykova, T.Y.; Zhimulev, I.F.; Belyaeva, E.S. Late replication domains are evolutionary conserved in the *Drosophila* genome. *PLoS One*, **2013**, *8*(12), e83319. Available from: journals.plos.org/plosone/article?id=10.1371/journal.pone.0083319

[29] Nordman, J.; Li, S.; Eng, T.; Macalpine, D.; Orr-Weaver, T.L. Developmental control of the DNA replication and transcriptional programs. *Genome Res*., **2011**, *21*(2), 175-181.

[30] Ho, J.W.; Jung, Y.L.; Liu, T.; Alver, B.H.; Lee, S.; Ikegami, K.; Sohn, K.A.; Minoda, A.; Tolstorukov, M.Y.; Appert, A.; Parker, S.C.; Gu, T.; Kundaje, A.; Riddle, N.C.; Bishop, E.; Egelhofer, T.A.; Hu, S.S.; Alekseyenko, A.A.; Rechtsteiner, A.; Asker, D.; Belsky, J.A.; Bowman, S.K.; Chen, Q.B.; Chen, R.A.; Day, D.S.; Dong, Y.; Dose, A.C.; Duan, X.; Epstein, C.B.; Ercan, S.; Feingold, E.A.; Ferrari, F.; Garrigues, J.M.; Gehlenborg, N.; Good, P.J.; Haseley, P.; He, D.; Herrmann, M.; Hoffman, M.M.; Jeffers, T.E.; Kharchenko, P.V.; Kolasinska-Zwierz, P.; Kotwaliwale, C.V.; Kumar, N.; Langley, S.A.; Larschan, E.N.; Latorre, I.; Libbrecht, M.W.; Lin, X.; Park, R.; Pazin, M.J.; Pham, H.N.; Plachetka, A.; Qin, B.; Schwartz, Y.B.; Shoresh, N.; Stempor, P.; Vielle, A.; Wang, C.; Whittle, C.M.; Xue, H.; Kingston, R.E.; Kim, J.H.; Bernstein, B.E.; Dernburg, A.F.; Pirrotta, V.; Kuroda, M.I.; Noble, W.S.; Tullius, T.D.; Kellis, M.; MacAlpine, D.M.; Strome, S.; Elgin, S.C.; Liu, X.S.; Lieb, J.D.; Ahringer, J.; Karpen, G.H.; Park, P.J. Comparative analysis of metazoan chromatin organization. *Nature*, **2014,** *512*(7515), 449-452. Available from: www.nature.com/articles/nature13415

[31] Beermann, W. Riesenchromosomen. In: *"Protoplasmatologia". 6/D;* Springer: Wien, **1962,** pp. 1-161.

[32] Berendes, H.D. Salivary gland function and chromosomal puffing patterns in *Drosophila hydei*. *Chromosoma*, **1965**, *17*(1), 35-77.

[33] Ashburner, M. Patterns of puffing activity in the salivary gland chromosomes of *Drosophila*. I. Autosomal puffing patterns in a laboratory stock of *Drosophila melanogaster*. *Chromosoma*, **1967**, *21*(4), 398-428.

[34] Crick, F. General model for the chromosomes of higher organisms. *Nature,* **1971,** *234*(5323), 25-27. Available from: https://link.springer.com/article/10.1038/234025a0

[35] Paul, J. General theory of chromosomes structure and gene activation in eukaryotes. *Nature,* **1972**, *238*(5365), 444-446. Available from: https://link.springer.com/article/10.1038/238444a0

[36] Judd, B.H.; Shen, M.W.; Kaufman, T.C. The anatomy and function of a segment of the X-chromosome of *Drosophila melanogaster*. *Genetics,* **1972**, *71*(1), 139-156.

[37] Zhimulev, I.F. Genetic organization of polytene chromosomes. *Adv. Genet*., **1999,** *39*, 1-589. Available from: www.sciencedirect.com/science/article/pii/S0065266008604769